Scientific Contributions Oil & Gas, Vol. 48. No. 2, August: 161 - 179

SCIENTIFIC CONTRIBUTIONS OIL AND GAS
Testing Center for Oil and Gas
LEMIGAS

Journal Homepage:http://www.journal.lemigas.esdm.go.id
ISSN: 2089-3361, e-ISSN: 2541-0520

Development and Fabrication of A Pressure Swing Adsorption System Using Molecular Sieve 13x for Integrated CO_2 Capture and Electrochemical Conversion

Mitra Eviani[1,2], Tirto Prakoso[1], Dadan Kusdiana[2], Pramujo Widiatmoko[1], Ida Bagus Oka Lyong Budhatama[1], Setyo Yanus Sasongko[3], Aryan Fathoni Amri[3], Wibawa Hendra Saputera[1], and Hary Devianto[1]

[1]Department of Chemical Engineering, Bandung Institute of Technology
Ganesha Street No. 10, Bandung, West Java, 40132, Indonesia.

[2]Ministry of Energy and Mineral Resources
Ciledug Raya Kav. 109, South Jakarta, 12230, Indonesia.

[3]PT Aimtopindo Nuansa Kimia
Soekarno Hatta, Bandung, West Java 40212, Indonesia.

Corresponding author: mitra.eviani@esdm.go.id.

Manuscript received: April 23th, 2025; Revised: May 06th, 2025
Approved: May 14th, 2025; Available online: May 16th, 2025; Published: May 19th, 2025.

ABSTRACT - This study focuses on the development and performance evaluation of a Pressure Swing Adsorption (PSA) system utilizing molecular sieve Zeolite 13X for CO_2 capture. A fixed-bed reactor was designed and simulated with Aspen Adsorption to optimize adsorption conditions. The system, tested with a 24.75 L/min gas feed (10% CO_2, 90% N_2) at 30 °C and 6 bar, operated cyclically every 7 minutes. Simulation results recommended a reactor volume of 4.9 L (ID 102 mm × T/T 600 mm). Sensitivity analysis showed that adsorption capacity declined as CO_2 concentration increased, with CO_2 uptake decreasing from 24.75 L/min at 10%-mol to 8.44 L/min at 70%-mol. Key design parameters such as feed flow rate, intraparticle voids, bulk density, and particle size were also evaluated. A prototype was built based on simulation results and tested, achieving a 120 s breakthrough time and an optimal 60 s swing interval over 17 cycles. This work supports the future integration of PSA-based CO_2 capture with electrochemical CO_2 reduction (ECO_2R).

Keywords: CO_2 capture, pressure swing adsorption, gas adsorption, molecular sieve zeolite 13X.

How to cite this article:

Mitra Eviani, Tirto Prakoso, Dadan Kusdiana, Pramujo Widiatmoko, Ida Bagus Oka Lyong Budhatama, Setyo Yanus Sasongko, Aryan Fathoni Amri, Wibawa Hendra Saputera, and Hary Devianto, 2025, Development and Fabrication of A Pressure Swing Adsorption System Using Molecular Sieve 13x for Integrated CO_2 Capture and Electrochemical Conversion , Scientific Contributions Oil and Gas, 48 (2) pp. 161-179. DOI org/10.29017/scog.v48i2.1772.

INTRODUCTION

Carbon dioxide, known as one of the "greenhouse gases" resulting from the industrial combustion of fossil fuels, is a major contributor to global warming and climate change. According to IEA data, global CO_2 emissions increased by 1.3% in 2022 (up by 490 Mt) and 1.1% in 2023 (up by 410 Mt), dominated by coal emissions (IEA 2024). Various governments around the world have committed to and undertaken efforts to lower atmospheric CO_2 levels, often within frameworks that promote a closed-loop system involving reducing, reusing, recycling, and removing emissions. These collective actions aim to combat climate change and manage emissions more effectively.

Numerous studies have demonstrated the effectiveness of CO_2 capture through adsorption, particularly for managing post-combustion gas (Dantas et al. 2011; Lee & Park 2015; Song et al. 2015; Younas et al. 2016; Grande et al. 2017; Abdul Kareem et al. 2018; Sabri et al. 2023; Yu et al. 2023; Bahmanzadegan & Ghaemi 2024). Commonly employed methods include Pressure Swing Adsorption (PSA) or Temperature Swing Adsorption (TSA), utilizing zeolite as the adsorbent due to its high adsorption capacity, low energy requirements, cost-effectiveness, and well-established technology (Ko, Siriwardane & Biegler 2005; Liu, Chen & Gao 2017; Chen et al. 2021).

While research on CO_2 capture from industrial exhaust gas is growing, a significant gap remains in integrating CO_2 capture with CO_2 electroreduction to produce value-added chemical products. Currently, most CO_2 capture technologies are primarily focused on separating CO_2 from natural gas (Grande et al. 2017). On the other hand, CO_2 separation from flue gas, compared to natural gas, presents unique challenges due to the lower concentration of CO_2 (typically 13-15% for coal-fired plants and 3-4% for natural gas-fired plants) and the presence of impurities such as nitrogen, sulfur dioxide, and particulates (Hägg & Lindbråthen 2005; Merkel et al. 2013; Russo et al. 2018). These impurities can degrade the effectiveness of separation processes and require additional treatment steps. Additionally, flue gas is at a lower pressure, necessitating significant energy for compression to transport and store the captured CO_2. In contrast, CO_2 separation from natural gas streams generally deals with higher CO_2 concentrations and fewer impurities, making the process more straightforward and less energy-intensive (Herzog 1999). CO_2 capture from flue gas represents an approach to mitigate uncontrolled CO_2 emissions, which contribute to environmental, resource, and climate issues, known as the "greenhouse effect". To effectively support these efforts, it is crucial to develop a comprehensive strategic plan. Recent mapping studies in Indonesia have identified significant potential for CCS implementation, with total storage capacity from depleted reservoirs reaching almost 5,193 $MtCO_2$. At the same time, central regions like South Sumatra, West Java, East Java, and Kalimantan collectively emit over 40 $MtCO_2$ annually from industrial sources and possess substantial storage capacities connected via pipeline networks (Al Hakim et al. 2025). CO_2 emissions have the potential to be transformed into valuable fuels or chemical derivatives. Therefore, the capture and/or utilization of CO_2 (Carbon Capture Utilization, or CCU), including its conversion into valuable chemical products such as formic acid, is essential (Rumayor, Dominguez-Ramos & Irabien 2018; Aldaco et al. 2019).

There are several methods to capture CO_2 as explained below. Temperature Swing Adsorption (TSA) systems are generally more suitable for low-concentration CO_2 capture with low regeneration frequency. Chen et al. (2021) reported that TSA systems with internal heat exchangers can improve thermal efficiency, but suffer from longer cycle times compared to PSA.

Chemical Absorption Using Amine Solvents, especially with monoethanolamine (MEA), remains the most mature technology for CO_2 capture, achieving high CO_2 removal efficiencies (>90%) in commercial plants. However, it involves high thermal regeneration energy (around 3.1–4.0 GJ/ton CO_2), solvent degradation, and corrosion issues (Yu et al. 2023).

Membrane-Based CO_2 Separation: Membrane technology is an emerging alternative due to its modular design and low energy footprint. Merkel et al. (2013) proposed membrane-assisted selective exhaust gas recirculation for natural gas-fired power plants, achieving CO_2 purities over 90% with lower energy consumption than PSA under certain conditions.

While this study demonstrates the promising performance of a PSA system using Zeolite 13X for CO_2 capture, it is valuable to compare this approach with alternative technologies, particularly membrane separation, chemical absorption, and temperature

swing adsorption (TSA). Each method presents trade-offs in efficiency, cost, energy consumption, and scalability. Alternative approaches include natural zeolite impregnated with MDEA, achieving 5.152 mg CO_2/g adsorbent capacity (Adriany et al. 2023).

In this context, our study focused only on the capture of CO_2 from power plant exhaust gas. By improving the efficiency and scalability of CO_2 capture, this research aims to ensure that CO_2 can be effectively captured and easily converted into value-added chemical products. This approach will bridge the existing gap between CO_2 capture and utilization, facilitating transitions to the integrated CCU system in the future. This research develops CO_2 capture technology using an innovative and efficient adsorption method with molecular sieve (MS) Zeolite 13X. Known for its high selectivity to CO_2, MS Zeolite 13X is the most extensively studied adsorbent in CO_2 separation processes (Cavenati, Grande & Rodrigues 2004; Plaza et al. 2010; Abd et al. 2020). Although Zeolite 13X remains a standard material due to its cost-effectiveness and high CO_2 selectivity, recent studies suggest that amine-functionalized solid sorbents and MOFs (metal organic frameworks) may outperform traditional zeolites under moist or trace contaminant conditions (Bahmanzadegan & Ghaemi 2024). However, they often come at a higher synthesis cost and lower mechanical robustness, making Zeolite 13X a more practical choice for pilot-scale integration.

The research outcomes include both analysis and simulation, as well as the development of a CO_2 capture adsorber prototype. A sensitivity analysis was conducted to evaluate the impact of operating capacity, intraparticle voids, particle bulk density, and particle size of the adsorbent on adsorption duration in a fixed bed reactor. The analysis also identified the optimal operating capacity for a PSA system within a vessel measuring ID 102 mm x T/T 600 mm for different CO_2 concentrations in the feed gas. The adsorption performance and sensitivity analysis were conducted using the Aspen Adsorption simulation tool. The development of the CO_2 capture adsorber prototype serves to validate and assess the performance of the simulation model. Thus, this research represents an essential initial step in demonstrating the potential of an integrated CO_2 capture and electrochemical conversion system. It not only enhances the understanding of the process mechanisms and performance but also lays the foundation for developing industry-wide solutions to tackle CO_2 emissions and promote sustainable development.

METHODOLOGY

Setting up the simulation of adsorption

The research began with the development of a model based on data validation from previous laboratory-scale research using MS Zeolite 13X particles, conducted by industrial partners. MS Zeolite 13X is known for its high surface area, typically around 726 m^2/g (Zhou et al. 2013). It has a microporous structure with an effective pore diameter of 10 angstroms, allowing it to adsorb larger molecules compared to other zeolites (Zeolites & Allied Products Pvt. Ltd., no date). The morphology of Zeolite 13X is generally octahedral, and it exhibits excellent thermal stability (Zhou et al. 2013). The pore size distribution is optimized for high adsorption capacity and rapid mass transfer rates (Salahudeen 2022). After validating and fitting the data from the laboratory-scale research, process simulation and sensitivity analysis are performed using the Aspen Adsorption V11.0 simulation tool. The adsorption simulation scheme for CO_2 capture is shown in Figure 1. To prevent the introduction of water into the flue gas, the PSA system is equipped with a water trap.

The Toth isotherm model, equation 1, is used for data-fitting and the simulation. This model allows for fitting data to more variable operating conditions than the Langmuir or Freundlich models on porous adsorbents and incorporates aspects of the Sips model, also known as the Langmuir-Freundlich isotherm model, combining elements of both. The parameters k and n have specific values for each adsorbent-adsorbate pair, with n indicating the heterogeneity of the adsorbent. If n = 1, the Toth model aligns with the Langmuir model.

$$q_i = q_{max,i}\left(\frac{(K_iP)^n}{(1+K_iP)^n}\right)^{1/n} \quad (1)$$

Where q_i is adsorbent capacity ($mol \cdot kg^{-1}$), $q_{max,i}$ is the maximum adsorbent capacity, Ki is the Toth adsorption equilibrium constant, and P is the adsorbate concentration ($mol \cdot L^{-1}$). The parameters that were obtained from the data-fitting are shown in Table 1.

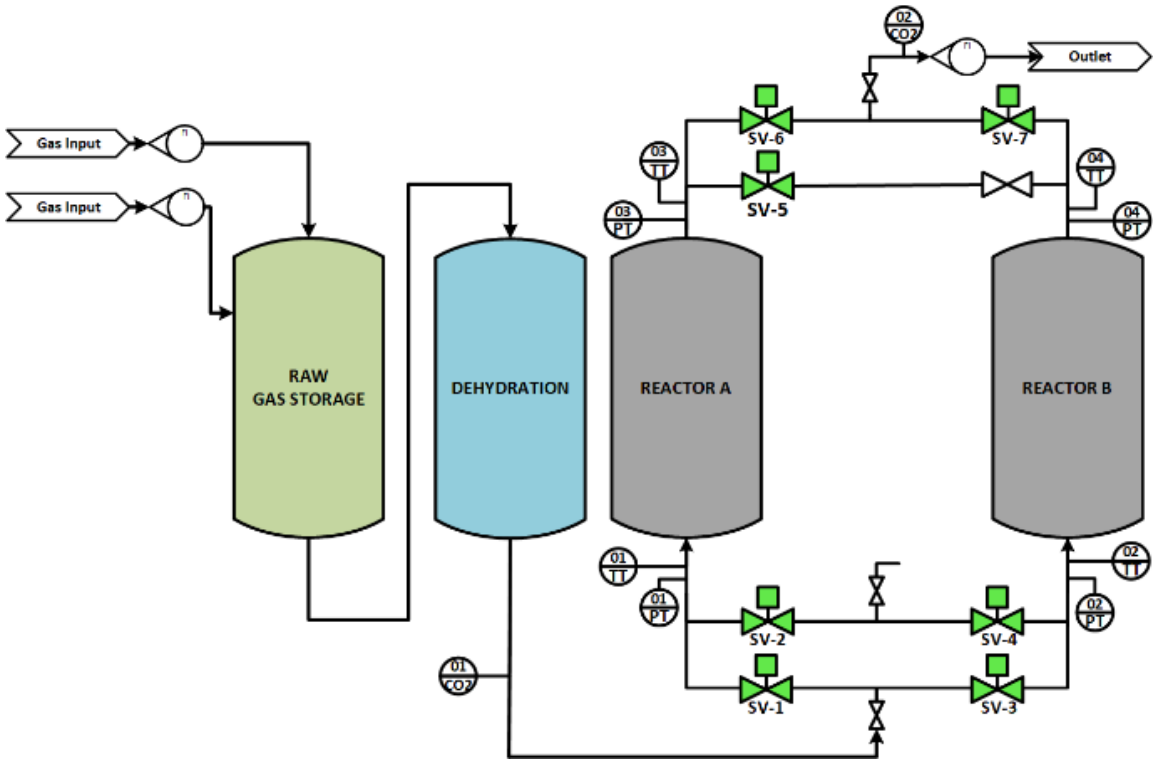

Figure 1. Schematic of CO_2 capture simulation.

Table 1. Toth model isotherm parameters used for simulation.

Parameter	CO_2	N_2	Units
$q_{max,i}$	5.05	2.21	mmol/g
K_i	0.73	0.07	bar^{-1}
n	1.20	0.56	

Aside from the mentioned isotherm model, there are other assumptions used for adsorption simulations, which include the use of the Peng-Robinson-Equation of State fluid package, known for its high accuracy in simulating hydrocarbon components; the use of MS Zeolite 13X as the adsorbent. These adsorbents were located inside an absorber column with an interparticle porosity of 0.42 m3·m-3 bed in the adsorber (with packed bed porosity ranging from 0.35 to 0.45 for columns with superior diameter to larger particle diameter ratios (Bahrun et al. 2022)); and a particle shape factor of 0.866 for cylindrical particles. The adsorption reactor is designed to handle gas feed samples according to the specifications in Table 2. For the design case, the absorber shall be capable of reducing the CO_2 content at the outlet to a maximum of 5% with 7 7-minute interval between swings. Subsequently, the CO_2 capture reactor design derived from the simulation was meticulously reviewed by the Engineering, Procurement, and Construction (EPC) company partners to fabricate a CO_2 capture reactor prototype ready for use.

Table 2. Gas feed sample specifications.

Parameter	Value	Unit
Temperature	30.0	^0C
Pressure	6.0	bar
Flowrate	24.75	L/min
CO_2 fraction	10.0	%-mol dry basis
N_2 fraction	90.0	%-mol dry basis

Sensitivity analysis of adsorber's capacity

A sensitivity analysis is conducted to determine the optimal operating capacity for the specified adsorption reactor on the CO_2 content in the feed gas at concentrations of 10, 30, 50, and 70%. The optimal operating capacity is determined based on the design

criteria, which have been mentioned previously (the absorber shall be capable of reducing the CO_2 content at the outlet to a maximum of 5% with 7 7-minute interval between swings).

Sensitivity analysis of adsorption performance

To observe the adsorber's performance (described as the interval between swings), a sensitivity analysis was conducted by varying four parameters: feed gas flow rate (0.35 – 20 L/h), intraparticle voids (0.2 – 0.8 m3/m3 particles), bulk density (300 – 900 kg/m3), and particle diameter (0.5 – 4 mm). In total, there is one base case as a design case and 14 sensitivity cases to rate the designed equipment. The list of cases is shown in Table 3.

been in the adsorption phase for 420 s (7 min). This result is achieved in an adsorber with a bed size of 4.9 L, with dimensions of ID 102 mm x T/T 600 mm. A Process Flow Diagram (PFD) of the CO_2 capture equipment can be arranged to resemble Figure 3.

Sensitivity analysis was conducted on the CO_2 content in the feed gas at concentrations of 10, 30, 50, and 70% to determine the optimal operating capacity for the specified adsorption reactor (vessel dimensions ID 102 mm x T/ T 600, swing interval every 7 min). Furthermore, the CO_2 capture reactor design derived from the simulation was meticulously reviewed by the Engineering, Procurement, and Construction (EPC) company partners to fabricate a CO_2 capture reactor prototype ready for use.

Table 3. List of adsorption cases.

Case No.	Feed Gas Flow Rate (L/min)	Intraparticle Void (m^3/m^3 particles)	Particles Bulk Density (kg/m^3)	Particles Diameter (mm)	CO_2 Content (%)	GHS V (h^{-1})
1 (Design)	24.75	0.2	500	1.49	10	10.88
2	0.35	0.2	500	1.49	70	0.15
3	1.00	0.2	500	1.49	70	0.44
4	5.00	0.2	500	1.49	70	2.20
5	20.00	0.2	500	1.49	70	8.79
6	0.35	0.4	500	1.49	70	0.21
7	0.35	0.6	500	1.49	70	0.31
8	0.35	0.8	500	1.49	70	0.62
9	0.35	0.2	300	1.49	70	0.15
10	0.35	0.2	700	1.49	70	0.15
11	0.35	0.2	900	1.49	70	0.15
12	0.35	0.2	500	0.50	70	0.15
13	0.35	0.2	500	1.00	70	0.15
14	0.35	0.2	500	2.00	70	0.15
15	0.35	0.2	500	4.00	70	0.15

RESULT AND DISCUSSION

Result of adsorber design

Figure 2 shows that the CO_2 content in the product gas reaches 5%-mol after the adsorber has

The effect of CO_2 concentration on adsorption capacity

Understanding the effect of CO_2 concentration on adsorption capacity is essential for optimizing the design of PSA systems, particularly for CO_2

capture applications. A sensitivity analysis was conducted to determine the adsorber capacity at CO_2 concentrations of 10, 30, 50, and 70% in the feed gas. These CO_2 concentrations were chosen based on the typical range found in flue gas from a 500 MW power plant, which contains between 13% and 21% CO_2 (Ho, Allinson & Wiley 2008; Monazam, Spenik & Shadle 2013). The higher concentrations were selected to assess the process sensitivity to variations in CO_2 concentrations. Compared to membranes, which typically exhibit lower selectivity in the presence of moisture or particulates and often require high feed pressure, making them less suitable for low-pressure flue gas compared to PSA systems (Merkel et al. 2013).

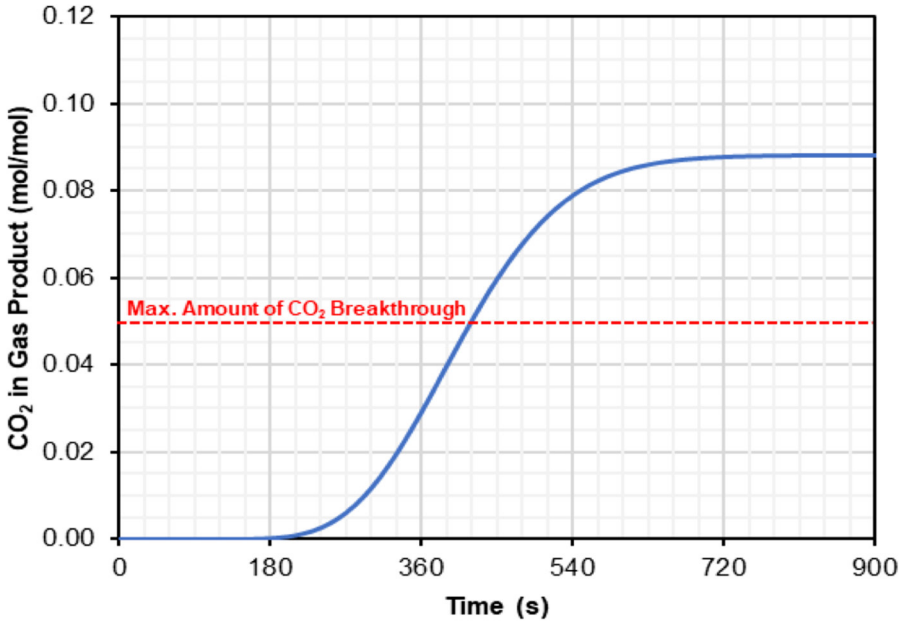

Figure 2. The performance of CO_2 capture reactor, ID 102 x T/T 600 mm, feed gas 24.75 L/min (10% CO2, 90% N2), 30 oC, 6 bar.

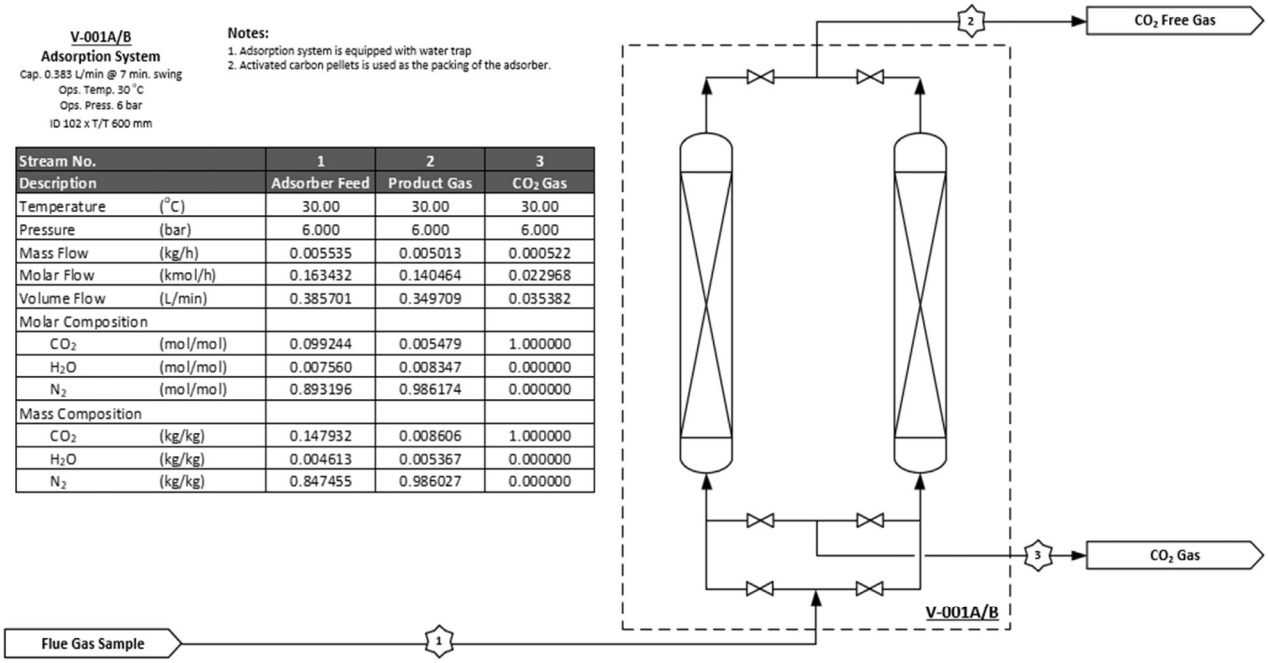

Stream No.		1	2	3
Description		Adsorber Feed	Product Gas	CO_2 Gas
Temperature	(°C)	30.00	30.00	30.00
Pressure	(bar)	6.000	6.000	6.000
Mass Flow	(kg/h)	0.005535	0.005013	0.000522
Molar Flow	(kmol/h)	0.163432	0.140464	0.022968
Volume Flow	(L/min)	0.385701	0.349709	0.035382
Molar Composition				
CO_2	(mol/mol)	0.099244	0.005479	1.000000
H_2O	(mol/mol)	0.007560	0.008347	0.000000
N_2	(mol/mol)	0.893196	0.986174	0.000000
Mass Composition				
CO_2	(kg/kg)	0.147932	0.008606	1.000000
H_2O	(kg/kg)	0.004613	0.005367	0.000000
N_2	(kg/kg)	0.847455	0.986027	0.000000

Figure 3. PFD of the designed CO_2 capture reactor.

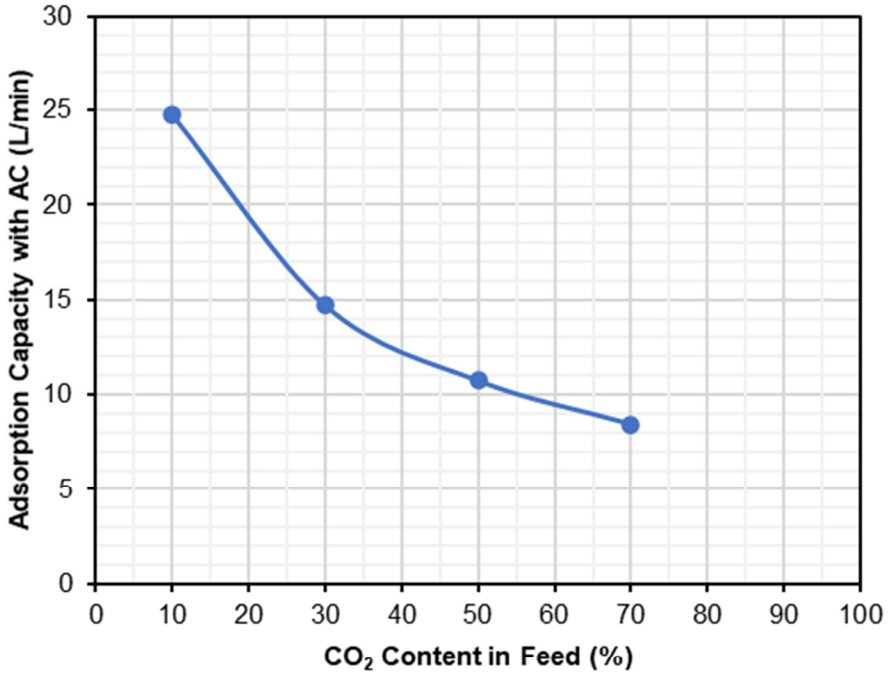

Figure 4. The effect of CO_2 concentration in feed gas on adsorption capacity @ 30 oC, 6 bar, εp = 0.2 m3·m-3 particles, ρs = 500 kg·m-3, dp = 1.49 mm, swing interval = 7 min.

Figure 4 shows that the capacity of the adsorption column with the MS increases from 8.44 L/min to 24.75 L/min as the CO_2 concentration in the feed gas decreases from 70% to 10%. Higher CO_2 content in the feed gas progressively limits the ability of the adsorbent to capture additional CO_2. Generally, at a constant flow rate, an increase in CO_2 concentration in the feed gas leads to a larger volume of CO_2 entering the adsorption column within a specific period, causing the adsorption column to reach saturation more quickly and thereby shortening the swing interval. This phenomenon occurs primarily due to intense competition among CO_2 molecules for available adsorption sites, causing the adsorbent to reach its maximum capacity more quickly (Ruthven 1984; Yang 2003).

Therefore, to maintain the same swing interval, the feed gas flow rate must be reduced at higher CO_2 concentrations. This adjustment helps to control the rate of saturation and extend the adsorption duration.

The effect of feed gas flow rate on interval swing adsorption

The analytical study of the breakthrough curve is fundamental to understanding the adsorption process. It offers insight into the behavior of the system and plays a key role in developing the dynamics of the adsorption column (Cen 1985). Figure 5 shows that within an adsorption system operating at 30 oC and 6 bar, the interval swing ranges from 170-180 s with a feed gas flow rate of 20 L/min to 10,180 s (almost three hours) with a flow rate of 0.35 L/min. PSA offers a cleaner and more energy-efficient alternative compared to a chemical absorption system, particularly when integrated with low-temperature processes like ECO_2R (Yu et al. 2023).

The longer swing interval in adsorption can be maintained at a lower feed gas flow rate because it takes more time for the particle bed to become saturated, as less CO_2 is adsorbed over a given period.

Meanwhile, the adsorption swing interval becomes shorter and the breakthrough curve sharper as the feed gas flow rate increases. With a higher flow rate, more unabsorbed gas passes through, leading to earlier saturation of the MS and increased CO_2 concentration at the outlet (Monazam et al. 2013). This indicates that the contact time between CO_2 and MS is reduced, preventing the MS from effectively capturing CO_2 and resulting in an earlier breakthrough time (Lu et al. 2022; Sabri et al. 2023). Higher flow rates also elevate operational costs due to the need for more frequent regeneration cycles. However, while a lower flow rate may maximize adsorption, it may be impractical for industrial applications where throughput is a significant consideration.

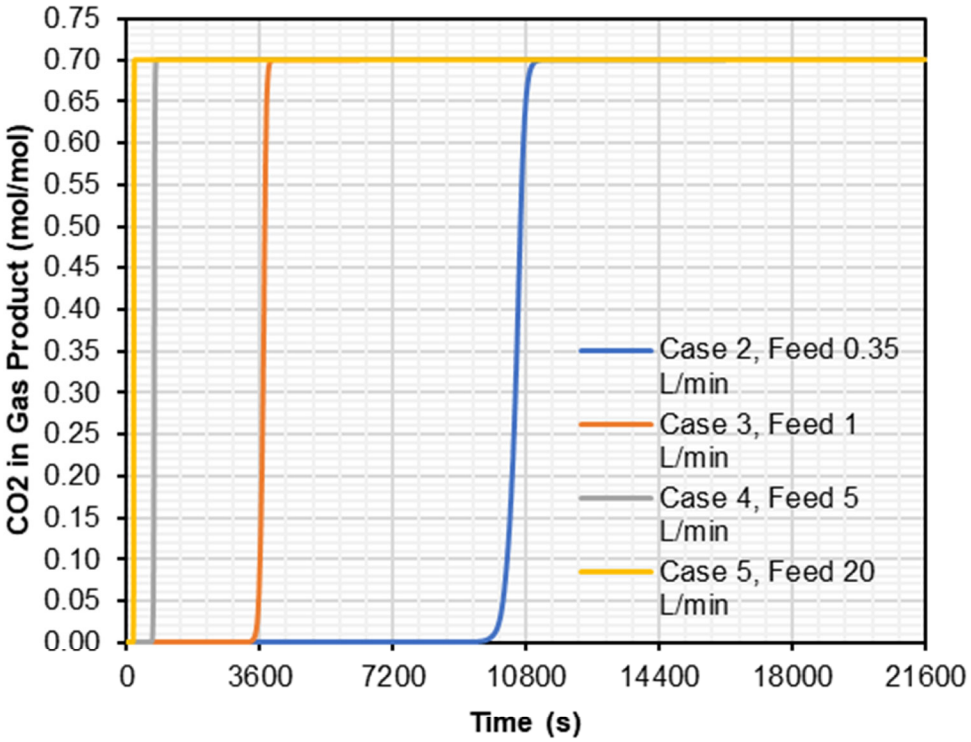

Figure 5. The effect of feed gas flow on CO_2 breakthrough @ 30 °C, 6 bar, feed gas 70% CO_2, ε_p = 0.2 m^3/m^3 particles, ρ_s = 500 kg/m^3, d_p = 1.49 mm.

The Effect of Intraparticle Voids on Interval Swing Adsorption

According to Figure 6, the interval swing time for adsorption is longer when particles with higher intraparticle voids (fewer solid particles) are used. This is attributed to particles with more intraparticle voids having a larger surface-to-volume ratio (Silva et al. 2022).

For two particles of identical volume but differing in intraparticle voids, the one with higher intraparticle voids possesses a larger surface area, providing a more effective surface for the adsorption reaction and thereby enhancing the adsorption capacity. In the adsorption system (30 oC, 6 bar, feed gas 0.35 L·min-1), the interval swing is 10,180 s with an intraparticle void of 0.2 m3/m3 particles. This interval swing extends to 10,450 s when the intraparticle void is increased to 0.8 m3/m3 particles, demonstrating that a larger pore volume results in increased adsorption. Particles with higher intraparticle voids have more pathways and spaces available for CO_2 to diffuse into, get adsorbed, and then be released during the desorption phase. This not only enhances the overall adsorption capacity but also potentially affects the kinetics of adsorption and desorption cycles.

In addition, sodium and potassium ions, as the principal cations of MS, play a significant role in CO_2 adsorption due to their strong interactions with CO_2 molecules (Hauchhum, Mahanta & De Wilde 2015). Na and K can alter the MS electronic environment and increase their affinity to CO_2 molecules, resulting in a high CO_2 adsorption capacity. Another researcher, Siriwardane, Shen & Fisher (2003), supports this, stating that natural zeolites with high sodium content showed high CO_2 adsorption capacity. This interaction is crucial in adsorption technology applications where selective adsorption of CO_2 is desired, such as in CCU.

The Effect of Bulk Density on Interval Swing Adsorption

As shown in Figure 7, the required interval swing is 6,270-6,280 s when the bulk density of MS particles is 300 kg/m3. The interval swing can extend up to 17,990 s (almost five hours) if the bulk density used is increased to 900 kg/m3. Within a fixed volume of the adsorber, a higher bulk density increases the volume (mass) of MS particles utilized, thereby enhancing the adsorption capacity.

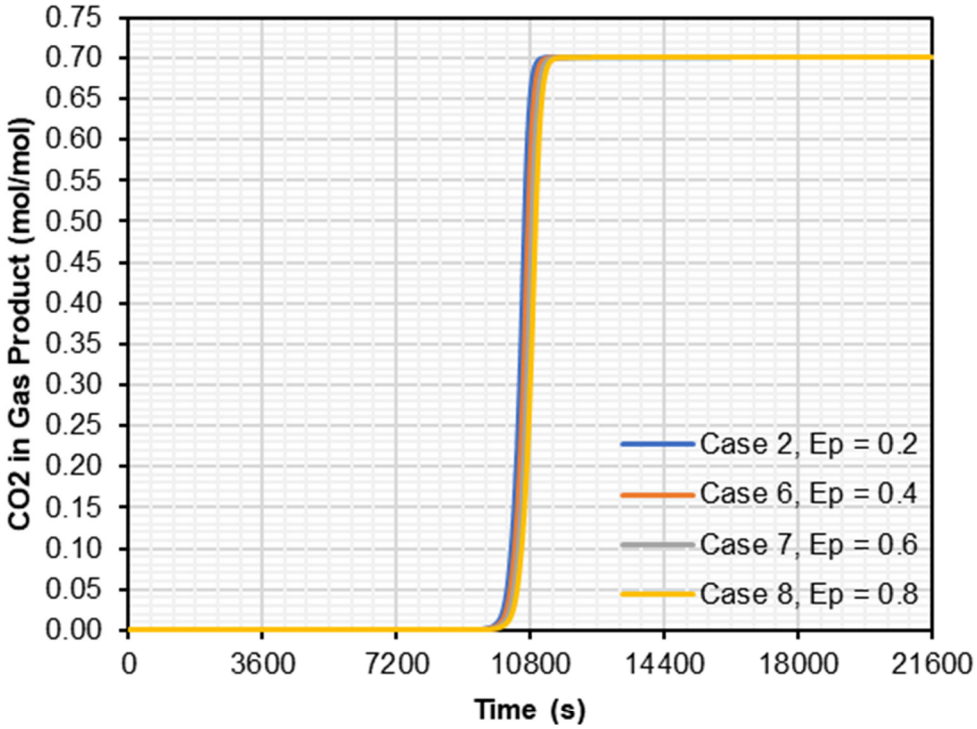

Figure 6. The effect of intraparticle voids on CO_2 breakthrough @ 30 °C, 6 bar, feed gas 70% CO_2, 0.35L/min, ρ_s = 500 kg/m^3, d_p = 1.49 mm.

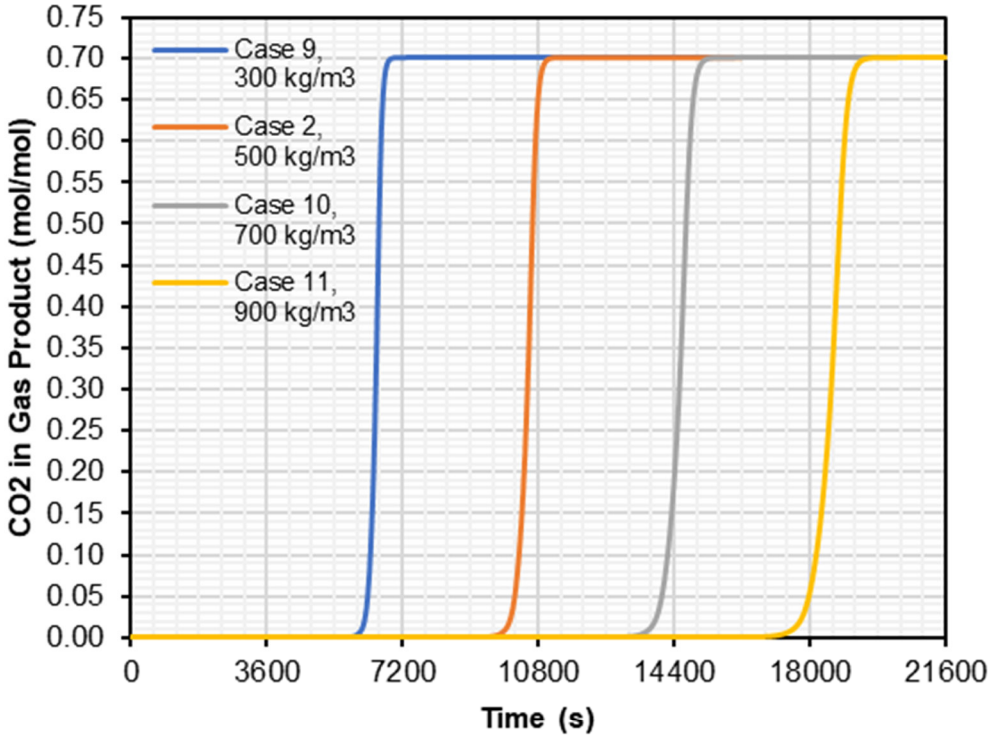

Figure 7. The effect of bulk density on CO_2 breakthrough @ 30 °C, 6 bar, feed gas 70% CO_2, 0.35L/min, ε_p = 0.2 m^3·m^{-3} particles, d_p = 1.49 mm.

A higher bulk density in MS implies a greater amount of adsorbent material in a fixed volume, which theoretically increases the total adsorption capacity due to the availability of more adsorption sites. However, this also reduces total porosity, potentially affecting the diffusion rate of gas molecules into MS pores. With higher density, gas molecules may take longer to penetrate (increasing flow resistance), impacting the dynamics of adsorption and desorption during the PSA cycle (Ruthven 1984). In addition, the influence of bulk density on thermal efficiency and MS regeneration should not be ignored. A denser adsorbent can lead to slower heat distribution during the regeneration phase, possibly requiring higher energy input or a more extended regeneration period to achieve effective desorption of the adsorbed gas (Yang 2003). This suggests that the system design must consider a trade-off between increasing adsorption capacity and operational regeneration efficiency. Analyzing and balancing these factors is crucial for the efficient design and operation of the PSA system.

The effect of particle size on interval swing adsorption

Based on Figure 8, different particle sizes affect the interval swing adsorption. As particle size increases, the interval swing becomes shorter, although the change is not significant. Research by Abdul Kareem et al. (2018) also indicates that pore size (microporosity) slightly contributes to the adsorption system. However, it was concluded that microporosity does not play a significant role in adsorption at low pressure. Furthermore, Yang et al. (2006) also concluded that microporosity, related to particle size, only slightly contributes to the adsorption system at low pressures.

Understanding the relationship between particle size and the mass transfer coefficient (MTC) is essential for analyzing trends in interval swings. In the adsorption system using MS, the MTC value is estimated by the Aspen Adsorption tool (Aspen Technology 2023). Eq. (2) shows that the MTC correlates linearly with the kinetic rate of adsorption.

$$\frac{\partial_q}{\partial_t} = MTC\ K_{Ki}(c_i - c_{i,max}) \quad (2)$$

where $\partial_q \cdot \partial_t^{-1}$ represent rate of adsorption. MTC is calculated using Eq. (3) and the Henry Coefficient (K_{Ki}) can be calculated using Eq. (4). Equation 3 describes MTC as a function of external film resistance, macropore diffusion, and micropore diffusion.

$$\frac{1}{MTC} = \frac{r_p}{3k_{fi}} + \frac{r_p^2}{15\varepsilon_p K_{pi}} + \frac{r_c^2}{15K_{Ki}^* D_{ci}} \quad (3)$$

$$K_{Ki} = \frac{\partial_{q_{max,i}}}{\partial c_i} = RT\frac{\partial_{q_{max,i}}}{\partial P_i} \quad (4)$$

In this context, r_p is particle diameter (m), rc is micropore diameter, k_f is external film resistance, ε_p is intraparticle porosity, K_p is macropore diffusion coefficient, D_c is micropore diffusion coefficient, K_k is Dimensionless Henry's law constant. Based on Eq. (3), particle diameter influences the MTC, with the MTC value decreasing as particle size increases, leading to a shorter interval swing. This concept aligns with the theory that larger particles have a smaller surface-to-volume ratio for gas-solid interactions, thereby reducing adsorption capacity. Zhou et al. (2015) also stated that larger particles exhibit greater intraparticle diffusion mass transfer resistance, which decreases with smaller particle size, resulting in improved intraparticle diffusion and adsorption rate for smaller particles.

Fabrication of CO_2 capture prototype

The simulation results were refined through collaboration and detailed reviews with the EPC vendor, resulting in the production of the CO_2 capture technology, as shown in Figure 9. The 3D design is shown in Figure 9(a). provides a detailed visualization and engineering precision of the CO_2 capture adsorber. Figure 9(b). further showcases the physical realization of a ready-to-use CO_2 capture prototype. Intensive collaboration with the EPC vendor is an important step in perfecting the adsorber design to ensure optimal performance and efficiency, as well as compliance with industrial standards.

In addition to the main prototype, the CO_2 capture system is complemented by control instrumentation. Figure 10 details a control panel equipped with an LCD-HMI (Human Machine Interface), facilitating user command and system monitoring. The instrumentation is also equipped with an online CO_2 analyzer, which is an essential component for real-time gas analysis. The analytical accuracy of this online CO_2 monitoring system has been validated against Gas Chromatography with Thermal Conductivity Detection (GC-TCD), a well-established reference method for CO_2 quantification

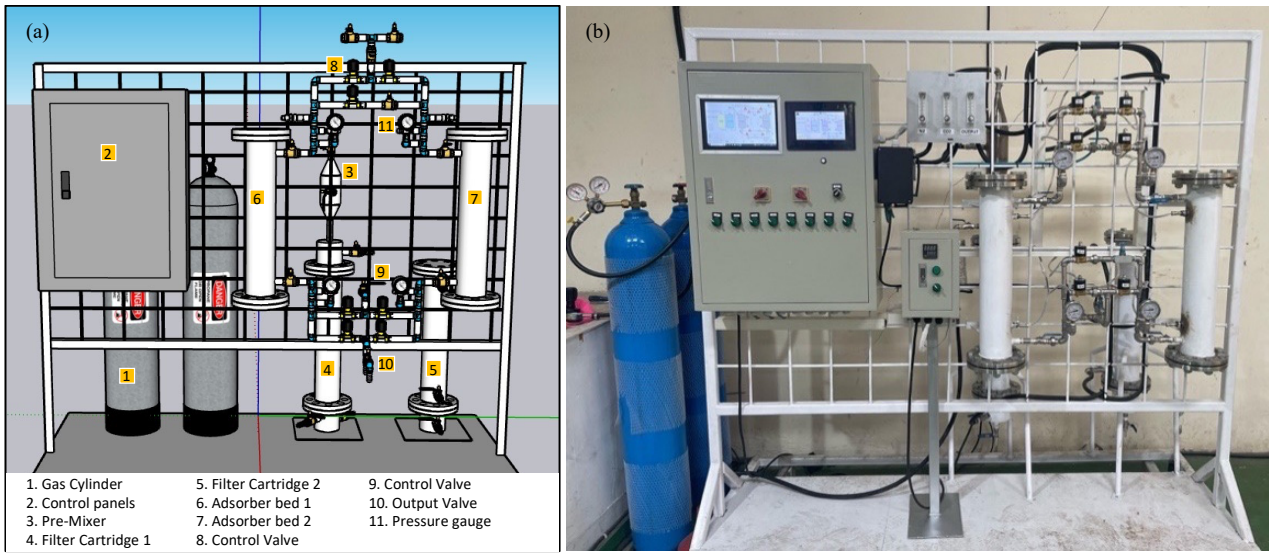

Figure 9. CO_2 capture prototype development: (a) 3D digital model showing system layout and component integration, (b) Physical prototype of the finalized CO_2 capture system.

Figure 10. (a). Control panels equipped with LCD-HMI, (b) instrumentation equipped with online CO_2 Analyzer

with intraday precision of 0.202% RSD and interday precision of 0.484% RSD, demonstrating acceptable accuracy within ±2σ bias limits (Mulyana et al. 2018). This GC-TCD validation approach follows ISO/IEC 17025 standards for simultaneous gas component measurement, ensuring reliable detection capabilities from ppm to percentage levels essential for optimizing CO_2 capture efficiency. The integration of these control and monitoring systems is necessary to ensure that the system operates within the desired parameters and achieves the highest capture efficiency, and maintains the standard required in engineering applications.

Performance test of CO_2 capture prototype

The breakthrough curve focuses on identifying the point when the adsorber reaches its capacity limit. In contrast, the interval swing adsorption curve provides insight into the adsorber's performance over repeated operational cycles, clearly illustrating the transitions between adsorption and desorption phases. By analyzing the characteristics of both the breakthrough and swing adsorption curves, the research offers a comprehensive understanding of the adsorber's performance in the CO_2 capture system. This thorough analysis aids in improving design and operational strategies, significantly advancing the efficiency of CO_2 capture technology. These advancements facilitate direct application in the power plant industry (tapping into the stack stream) and integration with an electrochemical CO_2 reduction (ECO_2R) system to produce formic acid. The CO_2 concentrations used in the feed gas are 25–30% with a flow rate of 15 L/min. The system is adjusted to perform a swing every 60 s. The swing interval is as low as 60 seconds, making PSA favorable for dynamic operation or integration with downstream conversion units such as ECO_2R (Chen et al. 2021).

With this configuration, the CO_2 is shown to be entirely adsorbed in the reactor, and no significant CO_2 content is measured at the outlet. Optimal performance test results were achieved with a duration of over 30 minutes (approximately 17 cycles) and an interval swing of 60 s, as shown in Figure 11.

A comparison of breakthrough curve of CO2 adsorption was made between the simulation results and the performance test results of the CO2 capture prototype.

The performance comparison was conducted with a breakthrough time of 120 seconds at a CO_2 feed concentration of 40% and an operating pressure of 8 bar. The performance comparison results are shown in Figure 12. The comparison between the simulation result and the prototype performance test results revealed discrepancies attributed to the non-ideal nature of the adsorption process. This discrepancy is a common challenge in CO_2 capture technologies, where real conditions often deviate from ideal simulations due to various factors such as material properties, operating conditions, and process complexities (Lu et al. 2023). The comparison between simulation and prototype performance test results of CO_2 capture technologies underscores the complexity of engineering applications and the importance of refining adsorption processes to bridge the gap between theoretical predictions and practical outcomes. By utilizing innovative materials and technologies tailored to specific operational requirements, advancements in CO_2 capture efficiency and effectiveness can be achieved.

Physicochemical properties were characterized using XRD to identify the main structure of the adsorbent. The X-ray diffraction (XRD) pattern of adsorbent indicate the similar pattern with molecular sieve (MS) Na-X dehydrated Zeolite 13X, Faujasite-type zeolite (FAU), as shown in Figure 13, exhibits characteristic peaks corresponding to its crystalline framework, with a dominant peak at a low 2θ values (2θ = 6.2, 10.1, 11.8, and 15.5◦), indicating a well-defined microporous structure and align well with the standard reference pattern for FAU pattern Joint Committee on Powder Diffraction Standards (JCPDS 12-0228). The presence of multiple peaks at higher angles further confirms the structural integrity and phase purity of the material. The peak intensities suggest a high degree of crystallinity, which is essential for maintaining a stable framework during adsorption applications (Thang et al. 2014).

Complementing the XRD results, the Brunauer-Emmett-Teller (BET) pore size distribution analysis, illustrated in Figure 14, reveals that the material possesses both microporous (<2 nm) and mesoporous (2–10 nm) regions.

The pore volume distribution curve indicates a significant contribution of mesopores within the 2–10 nm range, which facilitates better gas diffusion and enhances CO_2 uptake efficiency. In addition, the BET multi-point surface area is 444.847 m2/g, which represents a large surface area. This is particularly relevant in adsorption-based carbon capture applications, where an optimally balanced microporous-mesoporous structure improves both the initial adsorption rate and the overall adsorption capacity (Khoramzadeh, Mofarahi & Lee 2019).

Further characterization through N_2 physisorption isotherms, as shown in Figure 15, confirms that the material exhibits a Type IV isotherm, indicative of mesoporous materials, according to the International Union of Pure and Applied Chemistry IUPAC classification. The isotherm displays a gradual increase in nitrogen uptake at low relative pressures ($P/P_0 < 0.4$), followed by a more pronounced uptake

at higher relative pressures, particularly above P/Po = 0.8. This behavior suggests the presence of mesopores with slit-like or interconnected structures. The observed hysteresis loop, although present, does not exhibit a strong limiting adsorption at high P/Po, aligning with typical mesoporous materials. The combination of mesoporous and high surface area supports enhanced gas diffusion and CO_2 uptake efficiency, making this material promising for adsorption-based applications (Sing 1985; Thommes et al. 2015).

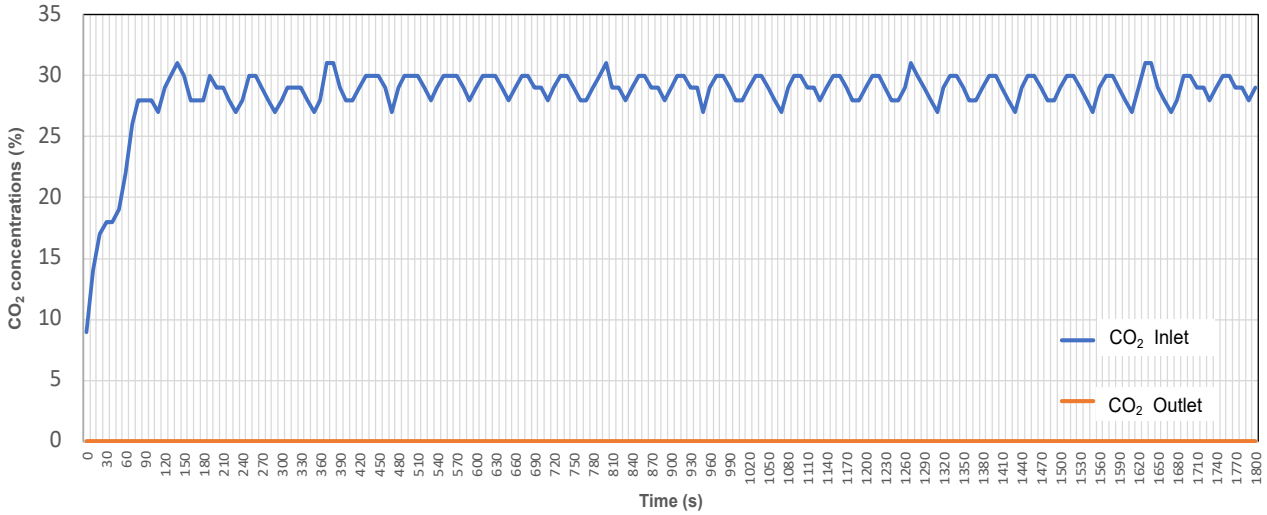

Figure 11. CO_2 concentration at inlet and outlet during PSA operation at optimal swing interval indicating efficient CO_2 adsorption.

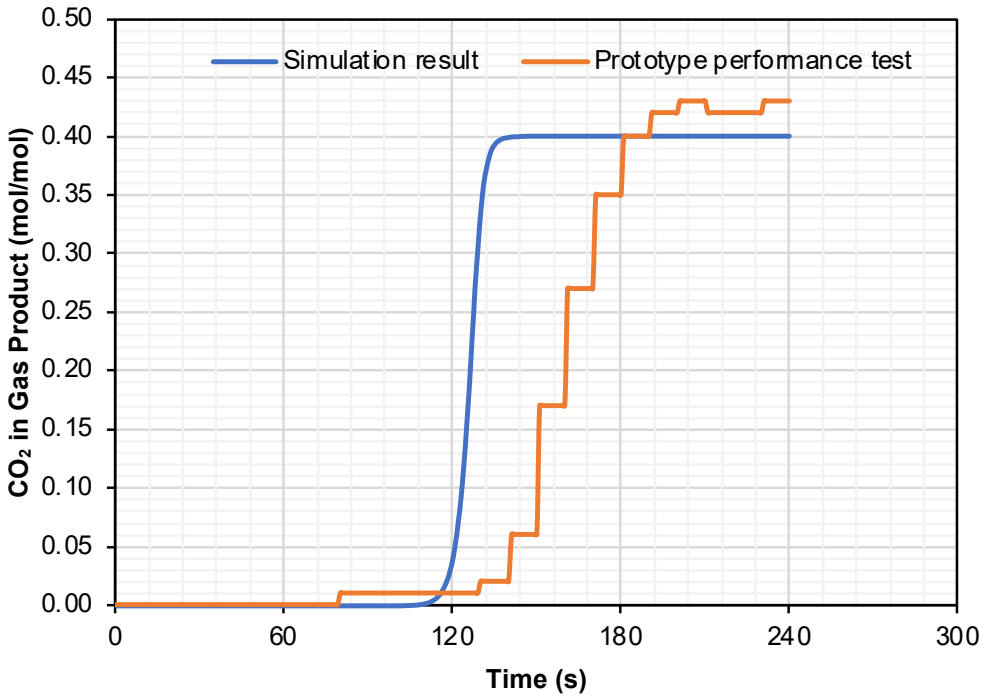

Figure 12. Breakthrough curve of CO_2 adsorption comparing simulation results and prototype performance.

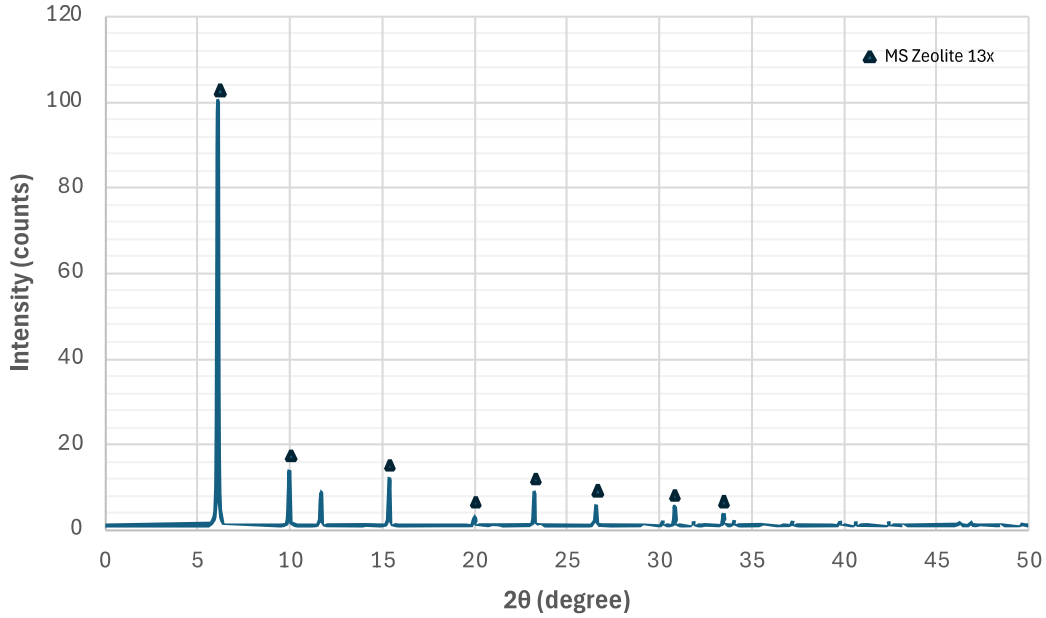

Figure 13. XRD pattern of MS Zeolite 13X (FAU structure, Na-X) in a good agreement with JCPDS 12-0228.

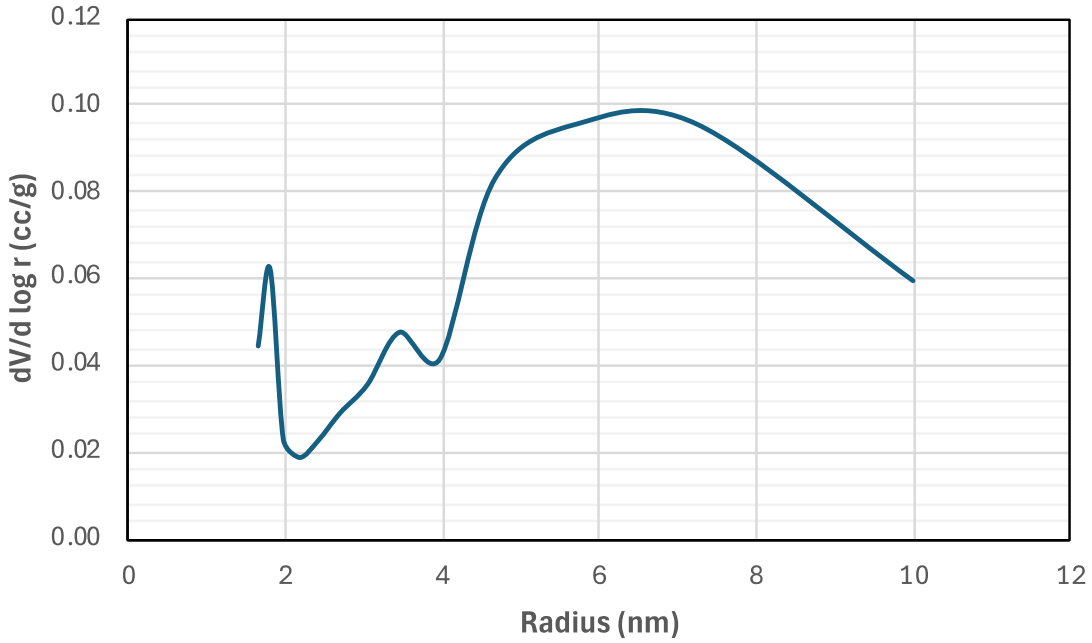

Figure 14. Pore size distribution of MS Zeolite 13X derived from N_2 adsorption–desorption analysis, showing predominant mesopores in the 5–10 nm radius range.

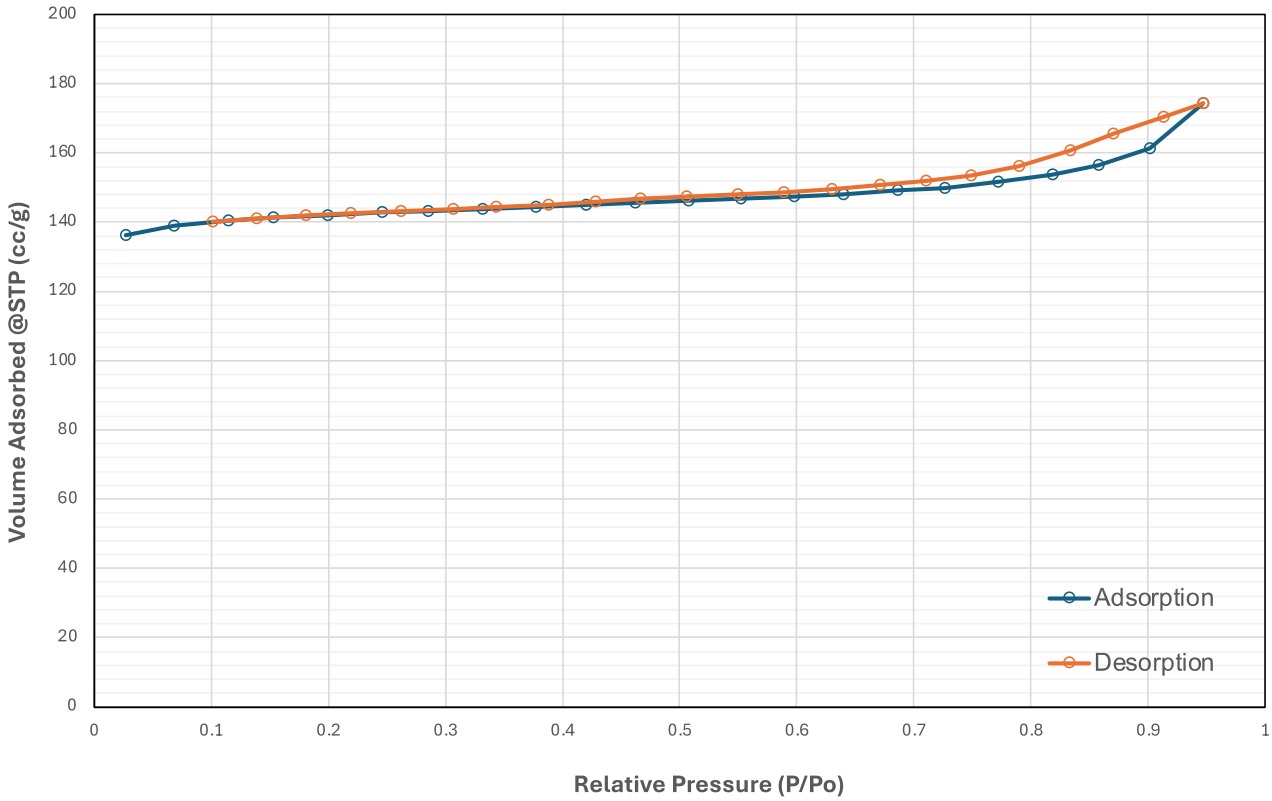

Figure 15. N_2 adsorption–desorption isotherm of MS Zeolite 13X showing a narrow hysteresis loop, indicating mesoporous structure and good reversibility of gas uptake at varying relative pressures.

The pore size distribution profile provides insight into the structural characteristics of the adsorbent material, which play a critical role in determining adsorption efficiency. Specifically, mesoporous structures within the range of 2–10 nm facilitate enhanced gas diffusion and improve CO_2 uptake capacity. The Interval Swing Adsorption Curve illustrates the temporal variation in CO_2 concentration during the adsorption process, serving as an indicator of the material's capacity to capture CO_2 effectively. The rapid initial increase observed in the curve suggests a high adsorption rate at the early stage, which is strongly dependent on the availability and accessibility of optimally sized pores (Siriwardane et al. 2001).

Additionally, the comparison between simulation and prototype performance tests provides an assessment of how experimental results align with theoretical predictions in CO_2 capture efficiency. Discrepancies between simulated and experimental data may arise due to variations in material properties, particularly non-uniform or suboptimal pore size distribution. A pore structure that is lower than 2 nm may restrict CO_2 diffusion, whereas huge pores higher than 10 nm may reduce the adsorbent's surface interactions, thereby diminishing overall adsorption efficiency. Consequently, the selection of adsorbent materials with well-optimized pore size distribution is essential for enhancing CO_2 capture performance, as evidenced by variations in CO_2 concentration throughout the process and the final comparative results between experimental and simulated data (Wang et al. 2014).

CONCLUSION

The design of CO_2 capture reactors was conducted through simulations using Aspen Adsorption V11.0. The CO_2 capture method employed adsorption with MS Zeolite 13X in a fixed-bed reactor. The reactor was designed to accommodate a gas feed of 24.75 L/min (10% CO_2, 90% N_2) at 30 °C and 6 bar, with swing operations in the PSA system occurring every 7 min. Simulation results indicated that the required reactor size is 4.9 L, with dimensions of ID 102 mm x H/T 600 mm. Sensitivity analysis revealed that the interval swing was longer with a lower gas feed flow rate (<20 mL/min); lower CO_2 concentration (<70%); the use of adsorbents with higher intraparticle voids (>0.2 m^3/m^3 particles), and the use of adsorbents with higher bulk particle density (>300 kg/m^3), while particle size had minimal impact on intervals swings.

In addition, the sensitivity analysis on the design of the adsorption reactor assessed the effect of CO_2 concentrations in the feed gas (10, 30, 50, and 70%-mol) on reactor capacity, resulting in capacities of 24.75 L/min for feed gas with 10%-mol CO_2, 14.69 L/min for 30%-mol CO_2, 10.73 L/min for 50%-mol CO_2, and 8.44 L/min for 70%-mol CO_2. To ensure that no water condensate forms on the gas sample, the adsorption reactor system is equipped with a water trap. The CO_2 capture reactor functioned properly according to the simulation-based design. The prototype was evaluated for operational performance and feasibility by analyzing breakthrough time and interval swing using feed gas containing 25-30% CO_2 and a flow rate of 15 L/min. Optimal performance test results were achieved with a duration of over 30 min (approximately 17 cycles) and an interval swing of 60 s. Optimizing the balance between the adsorption and desorption processes in PSA is crucial to prevent unwanted adsorbent saturation. This prototype will be integrated with an electrochemical CO_2 reduction (ECO_2R) system to convert CO_2 into formic acid using H-cell and PEM cells, aiming to create a holistic and effective system.

ACKNOWLEDGEMENT

We acknowledge the support of PT Pupuk Indonesia Utilitas under the grant Number 8877/IT1. C07KS/2023.

GLOSSARY OF TERMS

Symbol	Definition	Unit
BET	Brunauer-Emmett-Teller	
CCU	Carbon Capture and Utilization	
CCS	Carbon Capture and Storage	
ECO_2R	Electrochemical CO_2 Reduction	
EPC	Engineering, Procurement and Construction	
FAU	Faujasite-type zeolite, Na-X	
GC-TCD	Gas Chromatography with Thermal Conductivity Detection	
GHSV	Gas Hourly Space Velocity	
HMI	Human Machine Interface	
IUPAC	International Union of Pure and Applied Chemistry	
JCPDS	Joint Committee on Powder Diffraction Standards	
LCD-	Liquid Crystal Display Human	
HMI	Machine Interface	
MDEA	Methyl Diethanol Amine	
MEA	Monoethanolamine	
MOF	Metal-Organic Framework	
MS	Molecular Sieve	
MTC	Mass Transfer Coefficient	
PEM	Proton Exchange Membrane	
PFD	Process Flow Diagram	
PSA	Pressure Swing Adsorption	
RSD	Relative Standard Deviation	
TSA	Temperature Swing Adsorption	
XRD	X-ray Diffraction	

REFERENCES

Abd, A.A., Naji, S.Z., Hashim, A.S., & Othman, M.R., 2020, 'Carbon dioxide removal through physical adsorption using carbonaceous and non-carbonaceous adsorbents: A review', Journal of Environmental Chemical Engineering, 8(5), 104142.

Abdul Kareem, F.A., Shariff, A.M., Ullah, S., Mellon, N., & Keong, L.K., 2018, 'Adsorption of pure and predicted binary (CO_2:CH4) mixtures on 13X-Zeolite: Equilibrium and kinetic properties at offshore conditions', Microporous and Mesoporous Materials, 267, 221–234.

Adriany, R.A., Sakarani, D., Haris, A., Yenti, E., Herlina, L., Hidayati, N., Morina, M., Herizal, H., Atmoko, A.D., Suhartono, R. & Arief, R., 2023, 'Pembuatan Adsorben CO_2 Berbahan Dasar Zeolit Alam Yang Diimpregnasi Dengan Methyl Diethanol Amine Dan Uji Kapasitas Adsorpsi CO_2 Dengan Sistem Batch', Lembaran publikasi minyak dan gas bumi, 57(2), 8–17. https://doi.org/10.29017/LPMGB.57.2.1573.

Aldaco, R., Butnar, I., Margallo, M., Laso, J., Rumayor, M., Dominguez-Ramos, A., Irabien, A., & Dodds, P.E., 2019, 'Bringing value to the chemical industry from capture, storage and use of CO_2: A dynamic LCA of formic acid production', Science of The Total Environment, 663, 738–753.

Aspen Technology, 2023, Aspen Adsorption Help/Using Aspen Adsorption/Adsorption Reference and Strategy/Gas Dynamic Adsorption Models/Configure Gas Layer Form (gas).

Bahmanzadegan, F., & Ghaemi, A., 2024, 'Modification and functionalization of zeolites to improve the efficiency of CO_2 adsorption: A review', Case Studies in Chemical and Environmental Engineering, 9, 100564.

Bahrun, M.H.V., Bono, A., Zaini, M.A.A., Othman, N., & Saptoro, A., 2022, 'Dynamic performances of adsorbents in an industrial-sized packed bed column for lead ion removal', Biomass Conversion and Biorefinery.

Cavenati, S., Grande, C.A., & Rodrigues, A.E., 2004, 'Adsorption Equilibrium of Methane, Carbon Dioxide, and Nitrogen on Zeolite 13X at High Pressures', Journal of Chemical & Engineering Data, 49(4), 1095–1101.

Cen, P., 1985, A study on multicomponent, bulk gas mixture separation by pressure swing adsorption and on breakthrough curve, State University of New York at Buffalo .

Chen, L., Deng, S., Zhao, R., Zhu, Y., Zhao, L. & Li, S., 2021, 'Temperature swing adsorption for CO_2 capture: Thermal design and management on adsorption bed with single-tube/three-tube internal heat exchanger', Applied Thermal Engineering, 199, 117538.

Dantas, T.L.P., Luna, F.M.T., Silva, I.J., Azevedo, D.C.S. de, Grande, C.A., Rodrigues, A.E. & Moreira, R.F.P.M., 2011, 'Carbon dioxide–nitrogen separation through adsorption on activated carbon in a fixed bed', Chemical Engineering Journal, 169(1–3), 11–19.

Grande, C.A., Roussanaly, S., Anantharaman, R., Lindqvist, K., Singh, P. & Kemper, J., 2017, 'CO_2 Capture in Natural Gas Production by Adsorption Processes', Energy Procedia, 114, 2259–2264.

Hägg, M.-B. & Lindbråthen, A., 2005, 'CO_2 Capture from Natural Gas Fired Power Plants by Using Membrane Technology', Industrial & Engineering Chemistry Research, 44(20), 7668–7675.

Hakim, M.F. Al, Tony, B., Chandra, S., Nugraha, F.Y. & Nandiwardhana, D., 2025, 'Mapping The Potential CO_2 Source-Sinks for Carbon Capture Storage From Industry In Indonesia', Scientific Contributions Oil and Gas, 48(1), 121–133. https://doi.org/10.29017/scog.v48i1.1626.

Hauchhum, L., Mahanta, P. & Wilde, J. De, 2015, 'Capture of $$\hbox {CO}_{2}$$ CO 2 from Flue Gas onto Coconut Fibre-Based Activated Carbon and Zeolites in a Fixed Bed', Transport in Porous Media, 110(3), 503–519.

Herzog, H.J., 1999, 'The economics of CO2 capture', Greenhouse Gas Control Technologies 4, pp. 101–106, Elsevier.

Ho, M.T., Allinson, G.W., & Wiley, D.E., 2008, 'Reducing the Cost of CO_2 Capture from Flue Gases Using Pressure Swing Adsorption', Industrial & Engineering Chemistry Research, 47(14), 4883–4890.

IEA, 2024, CO_2 Emissions in 2023, Paris .

Khoramzadeh, E., Mofarahi, M., & Lee, C.-H., 2019, 'Equilibrium Adsorption Study of CO_2 and N_2 on Synthesized Zeolites 13X, 4A, 5A, and Beta', Journal of Chemical & Engineering Data, 64(12), 5648–5664.

Ko, D., Siriwardane, R., & Biegler, L.T., 2005, 'Optimization of Pressure Swing Adsorption and Fractionated Vacuum Pressure Swing Adsorption Processes for CO_2 Capture', Industrial & Engineering Chemistry Research, 44(21), 8084–8094.

Lee, S.-Y. & Park, S.-J., 2015, 'A review on solid adsorbents for carbon dioxide capture', Journal of Industrial and Engineering Chemistry, 23, 1–11.

Liu, F., Chen, S., & Gao, Y., 2017, 'Synthesis of porous polymer based solid amine adsorbent: Effect of pore size and amine loading on CO_2 adsorption', Journal of Colloid and Interface Science, 506, 236–244.

Lu, G., Wang, Z., Bhatti, U.H. & Fan, X., 2023, 'Recent progress in carbon dioxide capture technologies: A review', Clean Energy Science and Technology, 1(1).

Lu, J., Tang, J., Li, J. & Wang, S., 2022, 'The comparison of adsorption characteristics of CO_2/H_2O and N_2/H_2O on activated carbon, activated alumina, zeolite 3A and 13X', Applied Thermal Engineering, 213, 118746.

Merkel, T.C., Wei, X., He, Z., White, L.S., Wijmans, J.G., & Baker, R.W., 2013, 'Selective Exhaust Gas Recycle with Membranes for CO_2 Capture from Natural Gas Combined Cycle Power Plants', Industrial & Engineering Chemistry Research,

52(3), 1150–1159.

Monazam, E.R., Spenik, J. & Shadle, L.J., 2013, 'Fluid bed adsorption of carbon dioxide on immobilized polyethylenimine (PEI): Kinetic analysis and breakthrough behavior', Chemical Engineering Journal, 223, 795–805.

Mulyana, M.R., Zuas, O., Budiman, H., Simanungkalit, S. & Rinaldi, N., 2018, 'Simultaneous Measurement Of Syn-Gas Component (H_2, CO_2, CH_4, And CO) As Product Of Biomass Gasification By Using Validated Gc-Tcd Method', Scientific Contributions Oil and Gas, 41(1), 41–50. https://doi.org/10.29017/SCOG.41.1.73.

Plaza, M.G., García, S., Rubiera, F., Pis, J.J., & Pevida, C., 2010, 'Post-combustion CO_2 capture with a commercial activated carbon: Comparison of different regeneration strategies', Chemical Engineering Journal, 163(1–2), 41–47.

Rumayor, M., Dominguez-Ramos, A. & Irabien, A., 2018, 'Formic Acid Manufacture: Carbon Dioxide Utilization Alternatives', Applied Sciences, 8(6), 914.

Russo, G., Prpich, G., Anthony, E.J., Montagnaro, F., Jurado, N., Lorenzo, G. Di, & Darabkhani, H.G., 2018, 'Selective-exhaust gas recirculation for CO_2 capture using membrane technology', Journal of Membrane Science, 549, 649–659.

Ruthven, D.M., 1984, Principles of adsorption & adsorption processes, John Wiley & Sons, New York.

Sabri, N.H., Rani, N.H.A., Mohamad, N.F., Mohd Muhsen, N.A.S. & Md Zaini, M.S., 2023, 'Simulation of CO_2 capture for amine impregnated activated carbon - palm kernel shell (AC-PKS) adsorbent in pressure swing adsorption (PSA) using Aspen Adsorption', Materials Today: Proceedings.

Salahudeen, N., 2022, 'A Review on Zeolite: Application, Synthesis and Effect of Synthesis Parameters on Product Properties', Chemistry Africa, 5(6), 1889–1906.

Silva, F.G. da, Vasilakaki, M., Cabreira Gomes, R., Aquino, R., Campos, A.F.C., Dubois, E., Perzynski, R., Depeyrot, J. & Trohidou, K., 2022, 'A numerical study on the interplay between the intra-particle and interparticle characteristics in bimagnetic soft/soft and hard/soft ultrasmall nanoparticle assemblies', Nanoscale Advances, 4(18), 3777–3785.

Sing, K.S.W., 1985, 'Reporting physisorption data for gas/solid systems with special reference to the determination of surface area and porosity (Recommendations 1984)', Pure and Applied Chemistry, 57(4), 603–619.

Siriwardane, R. V., Shen, M.-S., & Fisher, E.P., 2003, 'Adsorption of CO_2 , N_2 , and O_2 on Natural Zeolites', Energy & Fuels, 17(3), 571–576.

Siriwardane, R. V., Shen, M.-S., Fisher, E.P. & Poston, J.A., 2001, 'Adsorption of CO_2 on Molecular Sieves and Activated Carbon', Energy & Fuels, 15(2), 279–284.

Song, C., Kansha, Y., Ishizuka, M., Fu, Q. & Tsutsumi, A., 2015, 'Conceptual design of a novel pressure swing CO_2 adsorption process based on self-heat recuperation technology', Chemical Engineering and Processing - Process Intensification, 94, 20–28.

Thang, H.V., Grajciar, L., Nachtigall, P., Bludský, O., Areán, C.O., Frýdová, E., & Bulánek, R., 2014, 'Adsorption of CO_2 in FAU zeolites: Effect of zeolite composition', Catalysis Today, 227, 50–56.

Thommes, M., Kaneko, K., Neimark, A. V., Olivier, J.P., Rodriguez-Reinoso, F., Rouquerol, J., & Sing, K.S.W., 2015, 'Physisorption of gases, with special reference to the evaluation of surface area and pore size distribution (IUPAC Technical Report)', Pure and Applied Chemistry, 87(9–10), 1051–1069.

Wang, J., Huang, L., Yang, R., Zhang, Z., Wu, J., Gao, Y., Wang, Q., O'Hare, D. & Zhong, Z., 2014, 'Recent advances in solid sorbents for CO_2 capture and new development trends', Energy Environ. Sci., 7(11), 3478–3518.

Yang, L., Dadwhal, M., Shahrivari, Z., Ostwal, M., Liu, P.K.T., Sahimi, M. & Tsotsis, T.T., 2006, 'Adsorption of Arsenic on Layered Double Hydroxides: Effect of the Particle Size', Industrial & Engineering Chemistry Research, 45(13), 4742–4751.

Yang, R.T., 2003, Adsorbents: Fundamentals and

Applications, John Wiley & Sons, Inc. , New Jersey.

Younas, M., Sohail, M., Leong, L.K., Bashir, M.J., & Sumathi, S., 2016, 'Feasibility of CO_2 adsorption by solid adsorbents: a review on low-temperature systems', International Journal of Environmental Science and Technology, 13(7), 1839–1860.

Yu, X., Catanescu, C.O., Bird, R.E., Satagopan, S., Baum, Z.J., Lotti Diaz, L.M., & Zhou, Q.A., 2023, 'Trends in Research and Development for CO_2 Capture and Sequestration', ACS Omega, 8(13), 11643–11664.

Zeolites & Allied Products Pvt. Ltd., no date, Technical Data Sheet (TDS) Molecular Sieve 13X.

Zhou, C., Alshameri, A., Yan, C., Qiu, X., Wang, H. & Ma, Y., 2013, 'Characteristics and evaluation of synthetic 13X zeolite from Yunnan's natural halloysite', Journal of Porous Materials, 20(4), 587–594.

Zhou, L., Qu, Z.G., Chen, L. & Tao, W.Q., 2015, 'Lattice Boltzmann simulation of gas–solid adsorption processes at pore scale level', Journal of Computational Physics, 300, 800–813.